International Research Journal of Advanced Engineering and Science
ISSN (Online): 2455-9024

Gold Geospatial Interpolations: Kriging versus Inverse Distance Weighting

Umar Sambo Umar[1], Abdulwahab Muhammad Bello[2], Zaara Munir[3]
[1]Department of Applied Geology, Abubakar Tafawa Balewa University, Bauchi, Nigeria
[2]Department of Geology, Gombe State University, Gombe, Nigeria
[3]Department of Earth Science, University of Ghana

***Abstract*— *The E-W oriented Julie belt is located in the central portion of North-Western Ghana. The Julie gold deposit is currently the highest-grade in NW Ghana. It is located in the Wa-East gold district, which lies within the Julie belt south of the Koudougou-Tumu granitoid domain. The overall aim of this work is to highlight the role of Univariate Geostatistics in geospatial modelling, this would permit the prediction of the gold anomalous zones in the study area and delineate zones or specific areas where more resources can be invested. A total of 1088 soil samples were collected from the study area on grid bases using soil auger drilling, these samples were analyzed for gold only using Au fire assay at the SGS laboratory Australia and the multi element distribution was determined using x-ray fluorescence. To achieve the estimations, predictions and interpolations, Kriging and Inverse Distance Weighting (IDW) were employed after logarithmic transformation. The effectiveness of these methods in geospatial modelling using geochemical data was indicated. The histograms indicated a positively skewed distribution which suggest the other variables (As, W and Pb) as pathfinders for gold (Au). Models produced from both methods with the log. transformed data indicated about two anomalous zones, one being at the center of the study area, and another around the eastern arm of the area. Since the gold was hosted within extensively sheared zones of the granitoids, it is logical that gold is identified around the eastern part of the area because secondary dispersion mechanism must have consistently taken place to alter the primary constituent.*

***Keywords*— *Geospatial Interpolations: Gold: Inverse Distance Weighting: Julie Belt: Krigin: Log. transformation.*

I. Introduction

The Julie gold deposit is currently the highest-grade in NW Ghana [1]. It is located in the Wa-East gold district, which lies within the Julie belt south of the Koudougou-Tumu granitoid domain. The Wa-East gold district also includes gold camps of Collette, Kjersti, Kandia, Julie west, Baayiri and Danyawu (Fig. 1).

The E-W oriented Julie belt is located in the central portion of North-Western Ghana and is bounded by the Koudougou-Tumu domain from the north, to the south by the Bole-Bulenga domain and to the east by the Bole-Nangodi belt. Bounded to the west of the Koudougou-Tumu domain is the Wa-Lawra belt. The Wa-Lawra belt is further divided into the eastern and western halves by the crustal scale Jirapa shear zone which usually exhibits sinistral characteristics [1]. The eastern half is composed of mainly 2139 ± 2 Ma (detrital zircon ages) metamorphosed sedimentary rocks (volcanosediments, greywackes, shales) and early syn-tectonic 2212 ± 1 Ma [2], [3] and 2153 ± 4 Ma [4] granitoids. These rocks have been intruded by the 2104 ± 1 Ma late kinematic granitoids [4], [5], [6], [3]. The rocks in the eastern half has experienced up to green schist metamorphism [6], [3]. The western half is composed of the 2187 ± 3 Ma mainly high-grade gneisses and granitoid [4]. These rocks here have been metamorphosed up to amphibolite facies.

The Julie belt is composed of low grade basalts, silicic volcano sediments and granitoids mostly with tonalitic affinities [1]. Dating done on the silicic volcano sediments showed that some of the rocks crystallized at 2129 ± 7 Ma [6], [3]. This indicates that some part of the belt formed at least at 2130 Ma. The foliation in volcanosediments and granitoids within this fault shows a stretching lineation plunging down-dip and towards higher grade rocks.

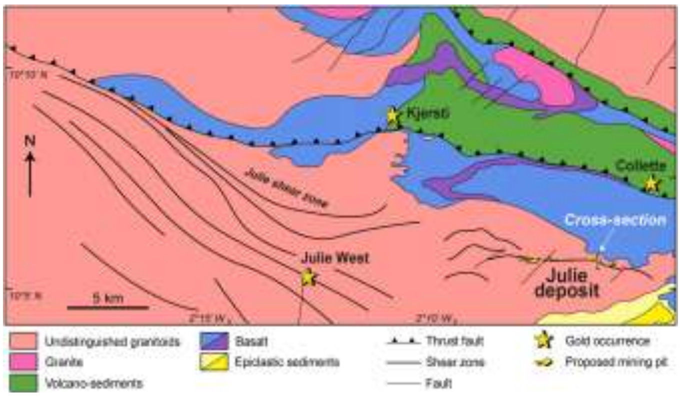

Fig. 1. Simplified map of the Julie belt. showing several mineralized occurrences in the Wa-East district [7]. The Julie deposit, in the lower right of the map, consists of several potentially exploitable workings.

II. Aim and Scope of the Study

The main target of geospatial modeling in this work is to predict the gold anomalous zones in the study area, to delineate zones or specific areas where more resources can be invested. Since the gold data, like most datasets used in the earth sciences, had spatial nature (taken from specific locations in the field), the exact geographical coordinates, the general trend, degree of continuity, general spatial representation are of significant interest in predictions. To achieve these estimations, predictions and interpolations, both methods of Kriging and Inverse Distance Weighting (IDW) were employed.

III. Methodology

Total of 1088 soil samples were obtained from the study area on grid bases using soil auger drilling method, this was

Umar Sambo Umar, Abdulwahab Muhammad Bello, and Zaara Munir "Gold Geospatial Interpolations: Kriging versus Inverse Distance Weighting.," *International Research Journal of Advanced Engineering and Science*, Volume 3, Issue 2, pp. 224-228, 2018.

made to an average depth of 3 m. These samples were analyzed for gold only at SGS laboratory Australia via Au fire assay. The multi element distribution was determined using x-ray fluorescence method. Kriging and Inverse Distance weighting (IDW) methods were employed to evaluate the spatial distribution of the gold. The plotting of the semi-variogram is the necessary step before Kriging [8], [9]. Semi variogram is a graphical device used to model the gold spatial continuity for the data set. The aim of kriging however is to estimate the value of the gold as a variable, at one or more unsampled points or over larger blocks, from more or less sparse sample data on a given support because the data may be distributed in one, two or three dimensions. The method can be used to locate mineralization [10]. IDW concept was derived from Shepard's method of spatial interpolation [11], the weight λ assigned to each of the known data points around the unknown area, is determined from the equation.

$$\lambda_i = \frac{\frac{1}{d_i^{\,p}}}{\sum_{i=1}^{n} \frac{1}{d_i^{\,p}}}$$

Where *d* is the distance between the unknown point and the closest data points, as is obvious from the equation, the value of λ is inversely proportional to the distance from the unknown data point. The exponent, *p*, is assigned to increase the weight of the closest points and decrease the influence of the farthest points, as a result, the higher the value of *p*, the greater is the difference between the farthest and closest points. As *p* approaches 0, the weights get more similar. This method has been proven effective for spatial analysis; e.g., [12], [13]. Statistical Package for Social Scientist (SPSS) was used for the descriptive statistics while Surfer 11.0 for the interpolations via kriging and IDW.

IV. Results and Discussion

A. The Descriptive Statistics

The raw geochemical data obtained was too large to be placed here, containing concentrations of 29 elements for the 1088 soil samples, but since this particular work is more of a univariate study, only four elements of interest were picked; the gold (Au) as the major variable upon which the geospatial analysis is conducted, and its already identified pathfinder elements which are Arsenic (As), Tungsten (W), and Lead (Pb) [14].

TABLE 1. Summary of descriptive statistics for the dataset before log. transformation.

	N	Range	Minimum	Maximum	Sum	Mean		Std. Deviation	Variance	Skewness		Kurtosis	
	Statistic	Statistic	Statistic	Statistic	Statistic	Statistic	Std. Error	Statistic	Statistic	Statistic	Std. Error	Statistic	Std. Error
Au_ppb	1088	2096	-2	2094	10671	9.81	2.172	71.640	5.132E3	23.732	.074	666.540	.148
As_ppm	1063	1698	0	1698	17501	16.46	2.274	74.151	5.498E3	14.199	.075	275.567	.150
W_ppm	1066	497	0	497	4272	4.01	.545	17.799	316.802	20.789	.075	556.454	.150
Pb_ppm	1087	88	0	88	7011	6.45	.130	4.275	18.279	7.179	.074	123.753	.148

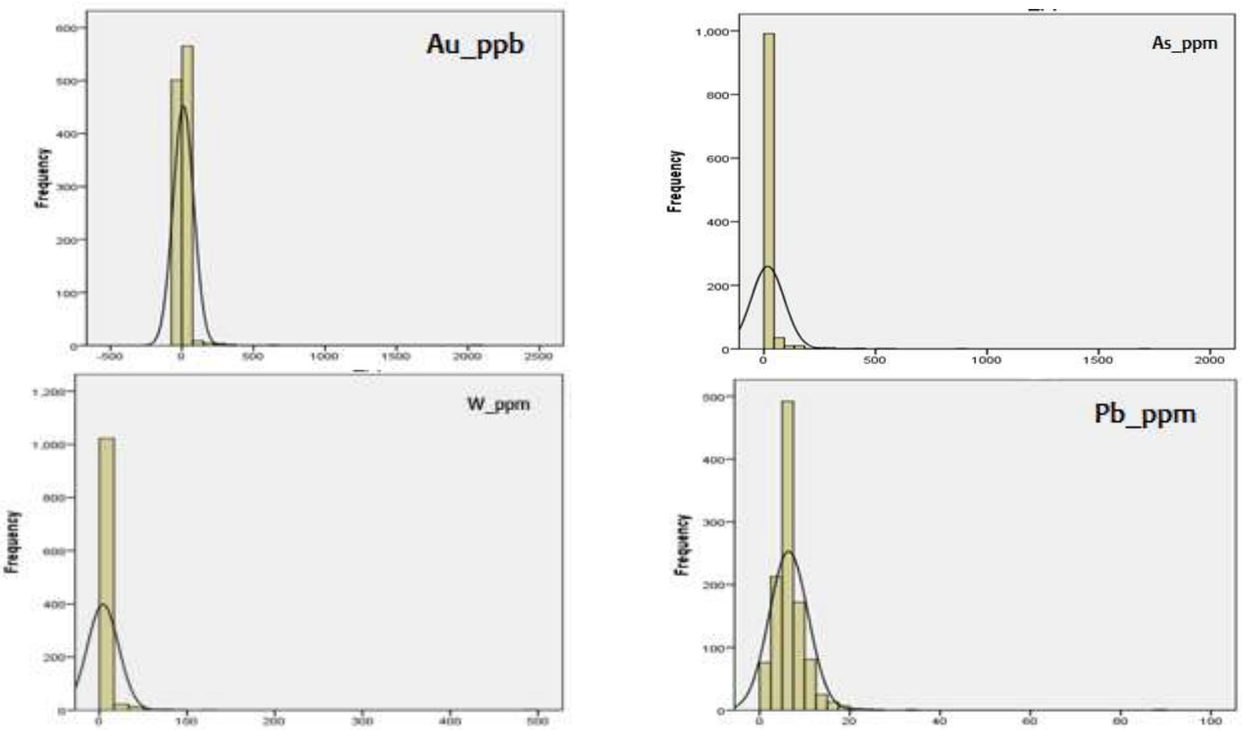

Fig. 2. Histogram plots before log. transformation.

International Research Journal of Advanced Engineering and Science
ISSN (Online): 2455-9024

The Summary of the descriptive statistics for the dataset was presented in Table 1. The variables (elements) have shown obvious disparity with the mean as 9.81, 16.46, 4.01 and 6.45 for Au, As, W, and Pb respectively. looking at their respective standard deviations, variance, skewness and kurtosis values, example the gold indicated a skewness value of 23.732 and a kurtosis of 66.540, these obvious disparity is the same with the remaining variables. Therefore, data have departed from the mean and are neither normally distributed nor stationary. This is an indication of the extreme variability of geochemical data [15].

The histograms plotted for these dataset (Fig. 2) further indicated that the data were neither normally distributed and nor are they stationary. The histograms have high kurtosis and were highly positively skewed (Fig. 2), the high kurtosis means that the concentrations of those respective elements were restricted to a particular portion of the study area which were represented by some particular samples in the laboratory analysis. The dataset has shown positive skewness also, and this means the concentrations of the elements in the study area is never uniform, majority of the samples will have averagely similar concentrations while some other few samples will have exceptionally high concentrations. Those samples may therefore represent point anomalies for the respective elements and the background concentrations may represent the background values for the respective element within the study area. According to [15], the very nature of geochemical data makes them rather spatially dependent and as such inherently non-normal.

Thus, logarithmic transformation was applied to the same dataset and the summary of the descriptive statistics is shown in table 2.

TABLE 2. Summary of descriptive statistics for the dataset after log. transformation

	N	Range	Minimum	Maximum	Sum	Mean		Std. Deviation	Variance	Skewness		Kurtosis	
	Statistic	Statistic	Statistic	Statistic	Statistic	Statistic	Std. Error	Statistic	Statistic	Statistic	Std. Error	Statistic	Std. Error
log_Au	587	3.32	.00	3.32	467.36	.7962	.02077	.50333	.253	1.187	.101	2.094	.201
log_As	633	3.23	.00	3.23	570.37	.9011	.02303	.57946	.336	.978	.097	.559	.194
log_W	254	1.92	.78	2.70	276.74	1.0895	.01624	.25885	.067	2.271	.153	7.217	.304
log_Pb	1022	1.64	.30	1.94	810.58	.7931	.00578	.18471	.034	.429	.077	1.727	.153

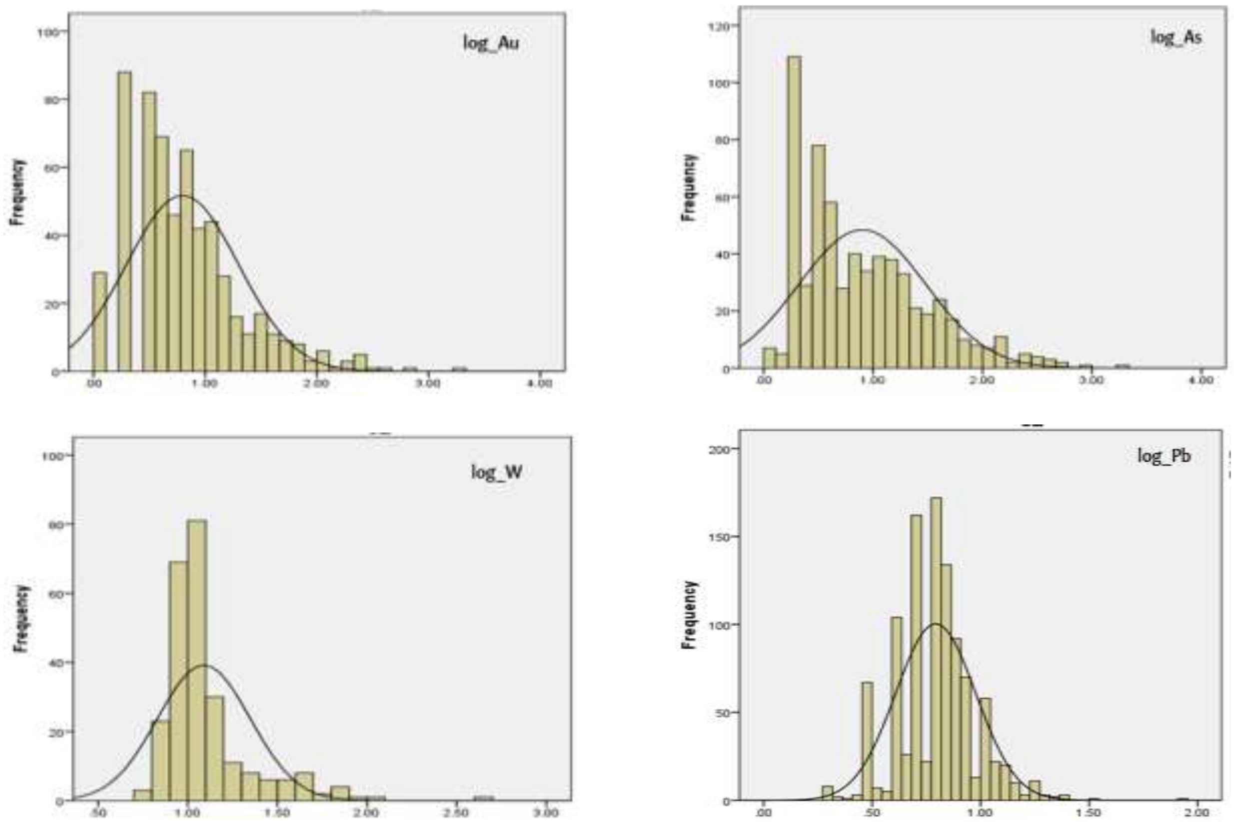

Fig. 3. Histogram plots after log. transformation.

Umar Sambo Umar, Abdulwahab Muhammad Bello, and Zaara Munir "Gold Geospatial Interpolations: Kriging versus Inverse Distance Weighting.," *International Research Journal of Advanced Engineering and Science*, Volume 3, Issue 2, pp. 224-228, 2018.

The difference between table 1 and 2 is undisputable, looking at the gold raw data for example, the number of observations for the Au has reduced down to 587 and this was because about 501 values were missing (below detection limit), the range here is 3.32 since the minimum value is 0.00 with the maximum value of 3.32. After the log_transformation, the mean is now 0.7962 instead of 9.81 before transformation. The standard deviation is now 0.5033 instead of 71.640 prior to transformation. The skewness and the kurtosis are now 1.187 and 2.094 respectively instead of 23.732 and 66.540 for both, before transformation. Indeed, the data has been transformed to near normal since the skewness and kurtosis of a normal distribution is 0 and 3 respectively. In fact, no dataset is exactly normally distributed, instead, it is only necessary for the data to be near normal [16]. Fig. 3; shows the histogram plots for the variables after the log_transformation, it further demonstrates how drastic the values had been justifiably transformed to better suit the univariate geospatial statistical analysis.

B. Gold Spatial Distribution

The methods of Kriging and Inverse Distance Weighting (IDW) were employed in analyzing the spatial distribution of the gold in the study area and to delineate the gold anomalous zones within. The method of Kriging is dependent on the type of theoretical model that best fit the semi variogram, Fig. 4 is the semi variogram fitted with gaussian curve. This was then used to generate the contour map in Fig. 5 and the 3d surface map in Fig. 6. However, Fig. 7 and 8 were generated using the method of IDW. This is important since it allows for comparison between the two results produced by each of the two distinct methods of geospatial modelling. It gives more confidence to the result.

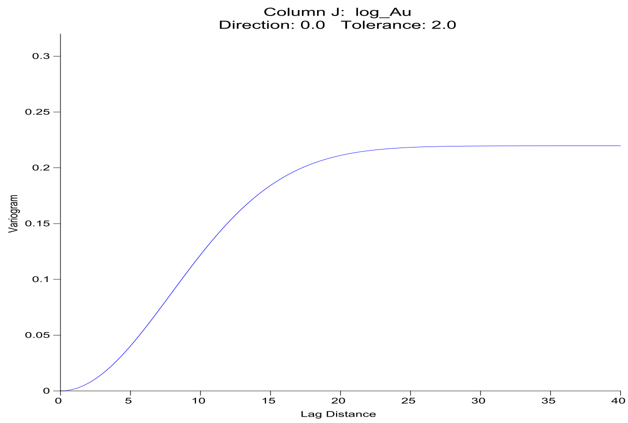

Fig. 4. Variogram plot for Au fitted with gaussian curve. From the Graph above, the following parameters were observed Nugget effect = 0, Range (a) = 20, Sill (C) = 0.23.

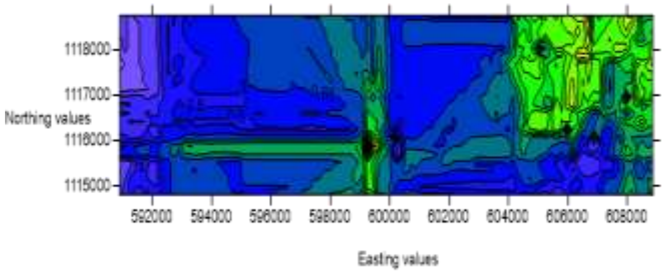

Fig. 5. Contour map for Au using Kriging.

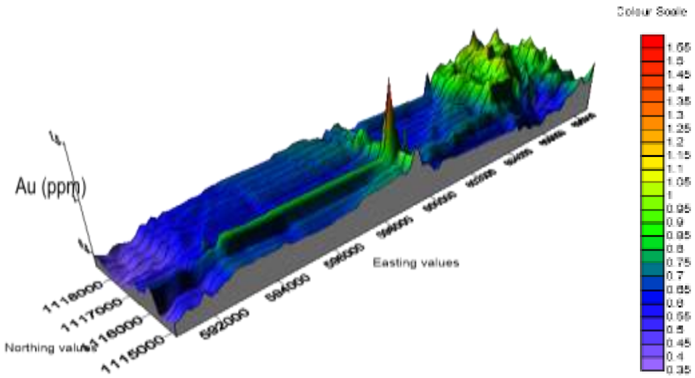

Fig. 6. 3d Surface map for Au using Kriging.

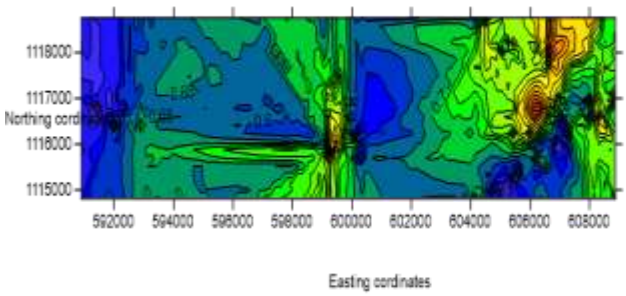

Fig. 7. Contour map for Au using IDW.

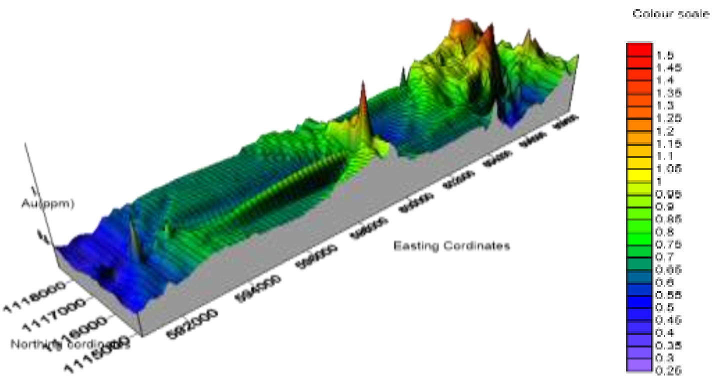

Fig. 8. 3d surface map for Au using IDW.

Kriging provides a solution to the problem of estimation based on a continuous model of spatial variation [17], [18]. In this case, it makes the best use of existing knowledge by taking account of the way the gold data varies in space through the variogram model.

From Fig.4, the gaussian model had values of 20 and 0.23 for the 'Range (a)' and the 'Sill (C)' respectively but a nugget value of 0, this indicated that there is no any nugget effect controlling estimations/predictions in the gridded maps as presented in Fig. 5 and 6 for 'contour' and '3d surface' maps respectively. From the color scale, the red color represents areas of higher gold concentrations and it degrades downward to the light blue color which represent areas having the lowest gold concentrations. This, therefore, indicated that the area having the highest gold concentration is within the center of the study area, since the Julie deposit is hosted in strongly sheared granitoids of the Julie belt [1], [3], [7], Meaning there is a conformity between what was earlier known with this result as obtained, and proves even better that the gold within the Julie belt is shear hosted and structurally controlled since the shear zone was also along the center of the study area.
Fig. 7 and 8 are the gridded 'contour' and '3d surface' maps respectively, generated by the method of Inverse Distance Weighting (IDW). Unlike Kriging, which bases its predictions on the semi-variogram, IDW bases its predictions on the exponent *'p'* which in this case a value of 2 was assigned, because '*p'* increases the weight of the closest points and decreases the influence of the farthest points. The result obtained conforms with what was earlier obtained via ordinary kriging, this has, to some extent indicated the robustness and simplicity of inverse distance interpolation which has motivated its continued use [19], [20].

V. CONCLUSION

The results obtained from both methods in analyzing the gold spatial distribution have shown no contradiction; indicating about two anomalous zones, one been at the center of the study area, and another around the eastern arm of the area. Since the gold was hosted within extensively sheared zones of the granitoids, it is logical that gold is identified around the eastern part of the area because secondary dispersion mechanism must have consistently taken place to alter the primary constituent. Both methods of Kriging and Inverse Distance Weighting (IDW) have therefore proven effective in modeling the gold spatial distribution within the Julie belt study area.

ACKNOWLEDGMENT

Azumah Resources Ghana Ltd and Department of Earth Science, University of Ghana are hereby acknowledged.

REFERENCES

[1] P. O. Amponsah, S. Salvi, D. Beziat, L. Sibernaller, L. Baratoux, M. W. Jessell, "Geology and geochemistry of the shear hosted Julie gold deposit, NW Ghana." *J. Afr. Earth Sci.B.*, 2015.
[2] P. A. Sakyi, B. X. Su, S. Anun, D. Kwasiyi, S. B. Dampare, C. Y. Anani, P.M. Nude, "New Zircon U-Pb ages for erratic emplacement of 2213-2130 ma Paleoproterozoic calc-alkaline I-type granitoid rocks in the lawra greenstone belt of Northwestern Ghana." *Precambrian Res*., 254. 140-168, 2014.
[3] X. Feng, P. O. Amponsah, R. Martina, J. Ganne, M. W. Jessell, "3-D numerical modelling of the influence of pre-existing faults and boundary conditions on the distribution of deformation: Example of NorthWestern Ghana." *Precambrian Res*, 2015.
[4] D. J. A gyei, G. K. Loh, K. O. Boamah, M. Baba, W. Hardes, M. Toloczyki, D. W. Davis. "Geological Mao of Ghana 1:1000000." Geol. Survey of Ghana (GSD), 2009.
[5] L. Baratoux, V. Metelka, S. Naba, M.W. Jessell, M. Gregoire, J. Ganne, "Paleoproterozoic crust evolution during the Eburnean orogeny (2.2 – 2.0 Ga) Western Burkina Faso." *Precambrian Res*., vol. 191, pp. 18-45, 2011.
[6] S. Block, J. Ganne, L. Baratoux, A. Zeh, L.A. Parra, M.W. Jessell, L. Aillers, L. Siebenaller, "Petrological and geochronological constraints on lower crust exhumation during Paleoproterozoic (Eburnean) orogeny, West African craton." *J. Metamorphic Geol*., vol. 33, pp. 463–494. 2015.
[7] S. Salvi, P.O. Amponsah, L.Siebeneller, D. Beziat, L. Baratoux, M. Jessell. "Shear – related gold mineralization in Northwestern Ghana: The Julie deposit." *Ore geology Rev*., vol. 78, pp. 712–717, 2015.
[8] S. Mukhopadhaya, "Rainfall Mapping using ordinary kriging technique: case study: Tunisia." *J. of Basic and Applied Engineering Res*., vol. 3, issue 1, pp. 1-5, 2016.
[9] N. Cressie, "Spatial prediction and ordinary kriging." *J. Mathematical Geol*, vol. 20, no. 4. 1988.
[10] J. E. Rosario, C.O. Mario, "Application of geostatistics to identify gold-rich areas in the Finisterre-Fervenza region, NW Spain." *Jour. Applied Geochemistry*, vol. 14, pp. 133–145, 1999.
[11] D. M. Louis, "Pollution models and inverse distance weighting: Some critical remarks." *Jour. Computers & Geosciences*, vol. 52, 2011.
[12] J. Stachelek, C. J. Madden, "Application of inverse path distance weighting for high density spatial mapping of coastal water quality patterns." *International Journal of Geographical Information Science*, 2015.
[13] L. Li, T. Losser, C. Yorke, R. Piltner, "Fast inverse distance weighting-based spatiotemporal interpolation: A web-based application of interpolating daily fine particulate matter PM 2.5 in the contiguous U.S. using parallel programming and k-d Tree." *Int. J. Environ. Res. Public Health*, vol. 11, pp. 9101-9141, 2014.
[14] U.S. Umar, P.M. Nude, P.O. Amponsah, A. I. Haruna, "Geostatistical analysis of gold multi-element associations using soil geochemical data from Julie Belt, Northwest Ghana." *International Journal of Mathematics and Physical Sciences Research*, vol. 4, issue 2, pp. 22-31, 2016.
[15] P. M. Nude, J. M. Asigri, S.M. Yidana, E. Arhin, G. Foli, J. M. Kutu, "Identifying pathfinder elements for gold in multi-element soil geochemical data from the Wa – Lawra Belt, Northwest Ghana: A multivariate statistical approach." *International Journal of Geosciences*, vol. 3, pp. 62-70, 2012.
[16] E. K. Baku, "Determination of Anomalous gold target by use of geochemical exploration and multivariate statistics methods in Chirano gold mining area of the western region, Ghana," M.S. thesis, Department of earth sciences, University of Ghana, Accra, Ghana, 2013.
[17] M. Balaban, B. Dengiz, "Lognormal ordinary kriging metamodel in simulation optimization." *Operations Research and Applications: An International Journal (ORAJ)*, vol. 5, no. 1, 2018.
[18] M. Jeihouni, R. Delirhasannia, S. K. Alavipanah, M. Shahabi, S. Samadianfard, "Spatial analysis of groundwater electrical conductivity using ordinary kriging and artificial intelligence methods (Case study: Tabriz plain, Iran)." *Geofizika*, vol. 32, 2015.
[19] O. Babak, C. V. Deutsch, "Statistical approach to inverse distance interpolation." *Stochastic Environmental Research and Risk Assessment*, vol. 23, issue 5, pp. 543-553, 2008.
[20] J. Zhou, Z. Sha, "A new spatial interpolation approach based on inverse distance weighting: Case study from interpolating soil properties." GRMSE 2013, Part II, CCIS 399, pp. 623–631, 2013.